The Gibbs-Free-Energy Landscape for Solute Association in Nanoconfined Aqueous Solutions (Postprint)

Authors: ZHAO Liang, WANG Chun-Lei, FANG Hai-Ping, TU Yu-Song

Date: 2023-06-18T00:00:00+00:00

Abstract

The theoretical model and the numerical analyses on the Gibbs-free-energy of the association states of amphiphilic molecules in nanoconfined aqueous solutions are presented in detail. We exhibit the continuous change of the Gibbs-free-energy trend, which plays a critical role in the association states of the system transforming from the dispersion state, through the "reversible state", and finally to the aggregation state in amphiphilic molecule solutions. Furthermore, for the "reversible state", we present the difference in the free-energy barrier heights of the dispersion state and aggregation state, resulting from the competition between the entropy, which makes the solute molecules evenly disperse in the solution and the energy contribution driving the amphiphilic molecules to aggregate into a larger cluster. These findings provide a comprehensive understanding of confinement effects on the solute association processes in aqueous solutions and may further improve the techniques of material fabrication.

Full Text

Preamble

The Gibbs-Free-Energy Landscape for Solute Association in Nanoconfined Aqueous Solutions

ZHAO Liang (赵亮),[1],[2] WANG Chun-Lei (王春雷),[1] FANG Hai-Ping (方海平),[1] and TU Yu-Song (涂育松)[3],†

[1]Division of Interfacial Water and Key Laboratory of Interfacial Physics and Technology, Shanghai Institute of Applied Physics, Chinese Academy of Sciences, Shanghai 201800, China
[2]University of Chinese Academy of Sciences, Beijing 100049, China

[3]College of Physics Science and Technology, Yangzhou University, Yangzhou 225009, China

(Received March 4, 2015; accepted in revised form April 20, 2015; published online June 20, 2015)

We present a detailed theoretical model and numerical analysis of the Gibbs free energy of association states of amphiphilic molecules in nanoconfined aqueous solutions. Our work reveals the continuous evolution of the Gibbs free energy landscape, which plays a critical role in the transformation of association states from dispersion, through a "reversible state," and finally to aggregation. For the reversible state, we demonstrate that the difference in free-energy barrier heights between the dispersion and aggregation states arises from competition between entropy—which drives uniform solute distribution—and energetic contributions that promote amphiphilic molecules to aggregate into larger clusters. These findings provide comprehensive insight into confinement effects on solute association processes in aqueous solutions and may advance material fabrication techniques.

Keywords: Gibbs-free-energy barrier, Dispersion, Aggregation, Nanoconfinement
DOI: 10.13538/j.1001-8042/nst.26.030504

Introduction

Solute association in aqueous solutions plays a fundamental role in diverse processes including crystal growth [?, ?], colloid particle nucleation [?, ?], surfactant micellization [?, ?], gas hydrate formation [?, ?], and biomolecule-related applications \cite{9–11}. When confined environments are involved—such as spaces between macromolecules in cells [?], pores in soil [?], or nanochannels in man-made nanomaterials [?, ?]—solute molecules exhibit behavior distinct from that in bulk solution. Zhang et al. [?] found that protein native-state stability can be enhanced at smaller confinement volumes, while Arai et al. [?] observed various morphologies during transitions in surfactant solutions confined in nanochannels. Additionally, Desarnaud et al. [?] reported the formation of a single skeleton crystal for sodium chloride at high supersaturation in confined geometry.

Our previous work [?] demonstrated that pentanol molecules can switch between dispersion and aggregation states—a phenomenon termed "reversible state transition"—in nanoconfined aqueous solutions using molecular dynamics simulations. We constructed an ideal physical model and numerically calculated the Gibbs free energy of a solute as a function of the number of molecules in a cluster. The unexpected observation was attributed to the presence of two minima separated by a maximum in the Gibbs free energy curve under confinement, with a free-energy barrier comparable to thermal fluctuations. Confinement also enhances the critical aggregation concentration because the limited solute number is insufficient to sustain a stable cluster at lower concentrations in the confined volume.

In our MD simulations, the pentanol molecule was described by the Gromos force field, where methyl or ethyl groups were treated as united atoms with implicit hydrogen atoms. This approach significantly accelerated computation to track dynamic association processes encompassing dispersion, reversible switching, and aggregation states. The packing of pentanol into clusters is minimally affected, as these groups behave as cohesive entities during aggregation, although a coarse description of water structure around methyl or ethyl groups results from the absence of explicit hydrogen atoms.

In this study, we first derive the free-energy formula based on an ideal physical model to elucidate the Gibbs free energy landscape of amphiphile association in nanoconfined geometry. Second, we specifically examine the Gibbs free energy barriers for dispersion and aggregation states in the reversible state and numerically investigate the relationship between barrier height and solute concentration. Finally, we summarize our conclusions regarding the characteristic reversible state behavior of amphiphilic solute association in nanoconfined aqueous solutions.

II. Model and Methods

A. Model of the Amphiphilic Molecule and Cluster

(1) A single amphiphilic alcohol molecule is modeled as a cuboid with a hydrophilic head and hydrophobic tail, as illustrated by the red and green geometry in Fig. 1(a). The molecule width, length, and tail length are denoted by a, L, and l, respectively, with molecular volume $v_m = a^{2L}$.

(2) A cluster consisting of densely packed amphiphilic molecules in water is treated as an ideal spherical aggregate [**?**] with radius $R(n)$:

$$R(n) = \left(\frac{3nv_m}{4\pi}\right)^{1/3} = \left(\frac{3na^{2L}}{4\pi}\right)^{1/3}$$

where n is the aggregation number (number of molecules in the cluster). The hydrophobic tails preferentially occupy the interior core while hydrophilic heads reside at the interfacial region exposed to water, as shown in Fig. 1(b)

.

B. Methods for Gibbs-Free-Energy Calculations

We introduce a theoretical description of Gibbs free energy to calculate the free energy of amphiphilic solute molecules in nanoconfined aqueous solutions. We consider that only a single cluster forms and that each solute molecule is either in the cluster or dispersed in solution. The total solute number is denoted by

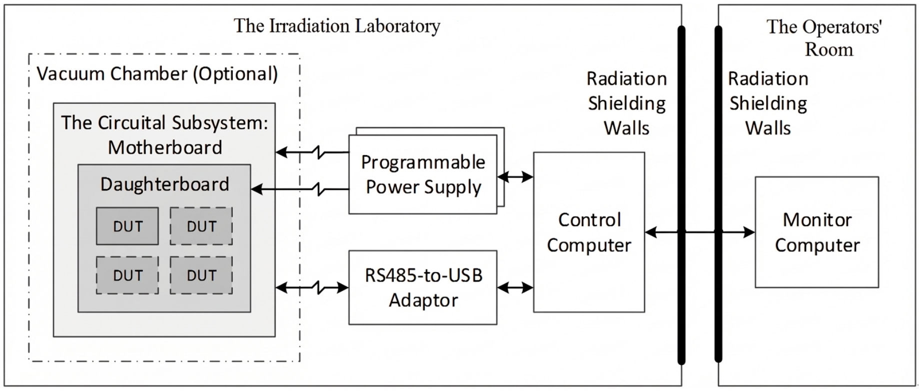

Figure 1: Figure 1

N, with $N-n$ molecules in the dispersed state. The Gibbs free energy G as a function of both cluster aggregation number n and solute number N is defined as:

$$\begin{aligned} G(n,N) = \Bigg\{ & 4\pi R(n)^2\gamma_{hw}^{\infty}\left[1-\frac{2\delta_{hw}}{R(n)}\right] \\ & + na^2\gamma_{w}^{\infty}\left[1-\frac{2\delta_{w}}{R(n)}\right] \\ & - na^2\gamma_{hw}^{\infty}\left[1-\frac{2\delta_{hw}}{R(n)}\right] \\ & + b\cdot k_{BT}n^{3/4} - n\cdot|\Delta\mu_{\text{transfer}}| \\ & + \Bigg[k_{BT}(N-n)\ln\left(\frac{N-n}{V-(N-n)v_w}\right) \\ & - k_{BT}(N-n) + B(N-n) \Bigg] \Bigg\} \end{aligned}$$

where k_B is the Boltzmann constant and T is the system temperature. The first three terms in curly braces represent surface energy contributions from hydrophobic tails, while the fourth term accounts for placing hydrophilic heads on the cluster surface. The term $n\cdot|\Delta\mu_{\text{transfer}}|$ represents the free energy difference for transferring a single hydrophobic tail from the dispersed phase into the hydrophobic core of the cluster. The terms in square brackets represent the free energy contribution from $N-n$ dispersed molecules. γ_{hw}^{∞} and γ_{w}^{∞} are interfacial tension coefficients for hydrophobic tail-water and water-vapor interfaces, respectively, while δ_{hw} and δ_w are the corresponding Tolman lengths [**?**]. Confinement effects are incorporated through V, the volume excluding the walls.

The relationship between cluster aggregation number n and total solute number

N, denoted $n(N)$, is derived by differentiating $G(n, N)$ with respect to n:

$$\begin{aligned}&\frac{1}{3}\gamma_{hw}^{\infty}\left[1-\frac{\delta_{hw}}{R(n)}\right]\left(\frac{3v_m}{4\pi}\right)^{1/3} n^{-2/3}\\&+\frac{b}{4}\cdot k_{BT} n^{-1/4}-|\Delta\mu_{\text{transfer}}|-B\\&=k_{BT}\ln\left(\frac{N-n}{V-(N-n)v_w}\right)\end{aligned}$$

where both sides represent the chemical balance between the cluster and dispersed molecules in confined aqueous solutions. By defining solute concentration $C = N/V$, we obtain expressions for $G(n, C)$ and $n(C)$ at fixed volume.

For numerical calculations, parameters were set as follows: $T = 300$ K; $V = 5.0\,\text{nm} \times 5.0\,\text{nm} \times 5.0\,\text{nm}$; for water, $\gamma_w^{\infty} = 72$ mN/m and $\delta_w = 1.23$ Å; for pentanol molecules, $\gamma_{hw}^{\infty} = 49.53$ mN/m, $a = 2.60$ Å, $l = 5.97$ Å, $b = 0.02$, and $-|\Delta\mu_{\text{transfer}}| - B = -5.26k_{BT}$. All numerical analyses were performed using Maple 18 software.

For a given amount of amphiphilic solute N in volume V, the Gibbs free energy $G(n, N)$ or $G(n, C)$ can be regarded as a function of cluster aggregation number n, denoted $G(n)$ for clarity. Local minima in $G(n)$ are found by $dG(n)/dn = 0$ and $d^{2G}(n)/dn^2 > 0$, while local maxima satisfy $dG(n)/dn = 0$ and $d^{2G}(n)/dn^2 < 0$. The barrier height G_{barrier} is defined as the magnitude of the Gibbs free energy difference between a local minimum and its adjacent maximum: $G_{\text{barrier}} = |G_{\max} - G_{\min}|$.

III. Results

To describe how many solute molecules aggregate into a cluster as solute concentration increases, we plot the $n(C)$ function based on Eq. (3). As shown in Fig. 2 [FIGURE:2], three concentration regions can be identified. When $C < 0.266$ mol/L, the aggregation number is $n \sim 1$, indicating no aggregates form and solute molecules remain dispersed. When sufficient solute is added ($C > 0.425$ mol/L), a distinct cluster emerges and grows larger with increasing concentration. Interestingly, in the intermediate "reversible state" region (0.266 mol/L $\leq C \leq$ 0.425 mol/L), the solute can exhibit both dispersion and aggregation states, as three aggregation numbers correspond to a given concentration. This bistability is clearly visible in the Gibbs free energy landscape shown in Fig. 3 [FIGURE:3].

Based on the Gibbs free energy formula in Eq. (2), we plot $G(n, C)$ curves at various concentrations. For $C = 0.266$ mol/L, only one minimum exists at $n \sim 1$, corresponding to the dispersion state. For $C = 0.439$ mol/L, the minimum at $n \sim 26$ indicates most molecules aggregate into a cluster. However, at $C = 0.279$ mol/L, $G(n)$ displays two minima at $n \sim 1$ and $n \sim 12$ separated by a maximum at $n \sim 4$. According to Eqs. (4) and (5), these correspond to stable dispersion, stable aggregation, and metastable states, respectively. This bistability also appears at $C = 0.332$ mol/L and 0.385 mol/L. The continuous evolution of the Gibbs free energy landscape with concentration is presented in Fig. 3(b) [FIGURE:3], which shows the surface colored by Gibbs free energy value. As concentration increases, the minimum corresponding to the dispersion state disappears while the aggregation state minimum emerges.

The emergence of minima and maxima at $C = 0.279$, 0.332, and 0.385 mol/L enables the system to switch between dispersion and aggregation states by overcoming the free-energy barrier through thermal fluctuations. This activation process depends directly on barrier height. Focusing on the reversible state region (0.266 mol/L $\leq C \leq$ 0.425 mol/L), Fig. 4 [FIGURE:4] shows the barrier heights for dispersion and aggregation states versus concentration, calculated using Eq. (6). The maximum barrier height is on the order of a hydrogen bond energy ($\sim 8k_{BT}$) in water at 300 K, allowing transitions between states under thermal fluctuations. Since energetic contributions driving aggregation dominate and larger clusters have lower free energy, the aggregation barrier height increases with concentration. The dispersion barrier height decreases, likely because the entropic effect promoting uniform solute distribution diminishes as concentration rises.

IV. Conclusion

In summary, we have presented a detailed derivation of the Gibbs free energy landscape describing amphiphilic solute association in nanoconfined aqueous solutions. Numerical calculations demonstrate that under confinement, as solute concentration increases, the free energy curve undergoes continuous transformation: from a single minimum at $n \sim 1$ (dispersion), through two minima separated by a maximum (reversible state), and finally to a single minimum at $n \sim N$ (aggregation). In the reversible state region, the maximum energy barrier is comparable to hydrogen bond energy ($\sim 8k_{BT}$), enabling switching between dispersion and aggregation states. We identified differences between dispersion and aggregation free-energy barriers, which arise from competition between entropy (promoting uniform distribution) and energy (driving cluster formation) as concentration increases.

Our work provides a comprehensive understanding of confinement effects on solute behavior in aqueous solutions. The theory is expected to be applicable to other amphiphilic molecules with more complex structures, such as peptides or surfactants, in nanoporous media or cellular environments—widely encountered confined systems.

References

[1] Piana S, Reyhani M and Gale J D. Simulating micrometre-scale crystal growth from solution. *Nature*, 2005, 438: 70–73. DOI: 10.1038/nature04173

[2] Myerson A S and Trout B L. Nucleation from solution. *Science*, 2013, 341: 855–856. DOI: 10.1126/science.1243022

[3] Kraft D J, Ni R, Smallenburg F, et al. Surface roughness directed self-assembly of patchy particles into colloidal micelles. *P Natl Acad Sci USA*, 2012, 109: 10787–10792. DOI: 10.1073/pnas.1116820109

[4] Chen Q, Whitmer J K, Jiang S, et al. Supracolloidal reaction kinetics of Janus spheres. *Science*, 2011, 331: 199–202. DOI: 10.1126/science.1197451

[5] Sanders S A, Sammalkorpi M and Panagiotopoulos A Z. Atomistic simulations of micellization of sodium hexyl, heptyl, octyl, and nonyl sulfates. *J Phys Chem B*, 2012, 116: 2430–2437. DOI: 10.1021/jp209207p

[6] Velinova M, Sengupta D, Tadjer A V, et al. Sphere-to-rod transitions of nonionic surfactant micelles in aqueous solution modeled by molecular dynamics simulations. *Langmuir*, 2011, 27: 14071–14077. DOI: 10.1021/la203055t

[7] Walsh M R, Koh C A, Sloan E D, et al. Microsecond simulations of spontaneous methane hydrate nucleation and growth. *Science*, 2009, 326: 1095–1098. DOI: 10.1126/science.1174010

[8] Debenedetti P G and Sarupria S. Hydrate molecular ballet. *Science*, 2009, 326: 1070–1071. DOI: 10.1126/science.1183027

[9] Hartgerink J D, Beniash E and Stupp S I. Self-assembly and mineralization of peptide-amphiphile nanofibers. *Science*, 2001, 294: 1684–1688. DOI: 10.1126/science.1063187

[10] Shityakov S and Dandekar T. Molecular dynamics simulation of popc and pope lipid membrane bilayers enforced by an intercalated single-wall carbon nanotube. *Nano*, 2011, 6: 19–29. DOI: 10.1142/s1793292011002317

[11] Shityakov S, Salvador E, Pastorin G, et al. Blood-brain barrier transport studies, aggregation, and molecular dynamics simulation of multiwalled carbon nanotube functionalized with fluorescein isothiocyanate. *Int J Nanomed*, 2015, 10: 1703–1713. DOI: 10.2147/IJN.S68429

[12] Homouz D, Perham M, Samiotakis A, et al. Crowded, cell-like environment induces shape changes in aspherical protein. *P Natl Acad Sci USA*, 2008, 105: 11754–11759. DOI: 10.1073/pnas.0803672105

[13] Perdrial N, Perdrial J N, Delphin J E, et al. Temporal and spatial monitoring of mobile nanoparticles in a vineyard soil: evidence of nanoaggregate formation. *Eur J Soil Sci*, 2010, 61: 456–468. DOI: 10.1111/j.1365-2389.2010.01263.x

[14] Gardeniers H J G E. Chemistry in nanochannel confinement. *Anal Bioanal Chem*, 2009, 394: 385–397. DOI: 10.1007/s00216-009-2672-5

[15] Tu Y S, Xiu P, Wan R Z, et al. Water-mediated signal multiplication with Y-shaped carbon nanotubes. *P Natl Acad Sci USA*, 2009, 106: 18120–18124. DOI: 10.1073/pnas.0902676106

[16] Zhang S Q and Cheung M S. Manipulating biopolymer dynamics by anisotropic nanoconfinement. *Nano Lett*, 2007, 7: 3438–3442. DOI: 10.1021/Nl071948v

[17] Arai N, Yasuoka K and Zeng X C. Self-assembly of surfactants and polymorphic transition in nanotubes. *J Am Chem Soc*, 2008, 130: 7916–7920. DOI: 10.1021/ja7108739

[18] Desarnaud J, Derluyn H, Carmeliet J, et al. Metastability limit for the

nucleation of NaCl crystals in confinement. *J Phys Chem Lett*, 2014, 5: 890–895. DOI: 10.1021/jz500090x
[19] Zhao L, Wang C L, Liu J, et al. Reversible State Transition in Nanoconfined Aqueous Solutions. *Phys Rev Lett*, 2014, 112: 078301. DOI: 10.1103/PhysRevLett.112.078301
[20] Prestipino S, Laio A and Tosatti E. Systematic improvement of classical nucleation theory. *Phys Rev Lett*, 2012, 108: 225701. DOI: 10.1103/PhysRevLett.108.225701